the FEBS Journal

Excess fructose intake-induced hypertrophic visceral adipose tissue results from unbalanced precursor cell adipogenic signals

María G. Zubiría[1], Juan P. Fariña[2], Griselda Moreno[3], Juan J. Gagliardino[2], Eduardo Spinedi[2] and Andrés Giovambattista[1]

1 IMBICE – Instituto Multidisciplinario de Biología Celular, Neuroendocrine Unit (CICPBA-CONICET LA PLATA), Argentina
2 CENEXA – Centro de Endocrinología Experimental y Aplicada (UNLP-CONICET LA PLATA), PAHO/WHO Collaborating Center for Diabetes, National University of La Plata School of Medicine, Argentina
3 LISIN – Laboratorio de Investigaciones del Sistema Inmune, National University of La Plata School of Exact Sciences, Argentina

Keywords
abdominal adipose tissue; adipogenic factors; leptin; lipid; SVF cells

Correspondence
E. Spinedi, CENEXA (UNLP-CONICET LA PLATA), Facultad de Ciencias Médicas UNLP, 60 y 120, 1900 La Plata, Argentina
Fax: +54 221 422 2081
Tel: +54 221 423 6712
E-mail: spinedi@cenexa.org

(Received 9 April 2013, revised 1 August 2013, accepted 29 August 2013)

doi:10.1111/febs.12511

We studied the effect of feeding normal adult male rats with a commercial diet supplemented with fructose added to the drinking water (10% w/v; fructose-rich diet, FRD) on the adipogenic capacity of stromal-vascular fraction (SVF) cells isolated from visceral adipose tissue (VAT) pads. Animals received either the commercial diet or FRD *ad libitum* for 3 weeks; thereafter, we evaluated the *in vitro* proliferative and adipogenic capacities of their VAT SVF cells. FRD significantly increased plasma insulin, triglyceride and leptin levels, VAT mass/cell size, and the *in vitro* adipogenic capacity of SVF cells. Flow cytometry studies indicated that the VAT precursor cell population number did not differ between groups; however, the accelerated adipogenic process could result from an imbalance between endogenous pro- and anti-adipogenic SVF cell signals, which are clearly shifted towards the former. The increased insulin milieu and its intracellular mediator (insulin receptor substrate-1) in VAT pads, as well as the enhanced SVF cell expression of Zpf423 and peroxisome proliferator receptor-γ2 (all pro-adipogenic modulators), together with a decreased SVF cell concentration of anti-adipogenic factors (pre-adipocyte factor-1 and wingless-type MMTV-10b), strongly supports this assumption. We hypothesize that the VAT mass expansion recorded in FRD rats results from the combination of initial accelerated adipogenesis and final cell hypertrophy. It remains to be determined whether FRD administration over longer periods could perpetuate both processes, or whether cell hypertrophy itself remains responsible for a further VAT mass expansion, as observed in advanced/morbid obesity.

Introduction

We have previously shown that the administration of a fructose-rich diet (FRD) to normal male rats for 3 weeks induces several metabolic and endocrine dysfunctions, such as hypertriglyceridaemia, impaired glucose tolerance, and high plasma leptin (LEP) and insulin levels, together with insulin resistance. In these

Abbreviations
ADIPOQ, adiponectin; AU, arbitrary units; CD, commercial diet; Ct, threshold cycle; Dd, differentiation day; FRD, fructose-rich diet; GR, glucocorticoid receptor; IRS-1, insulin receptor substrate-1; LEP, leptin; LG, low glucose; MR, mineralocorticoid receptor; Pd, proliferation day; PPAR, peroxisome proliferator receptor; Pref-1, pre-adipocyte factor-1; SVF, stromal-vascular fraction; TBARS, thiobarbituric acid reaction substances; VAT, visceral adipose tissue; Wnt, wingless-type MMTV.

animals, we also recorded a marked increase in visceral adipose tissue (VAT) mass and impairment of its metabolic and endocrine functions [1–3].

Adipose tissue (AT), particularly the VAT fraction, plays an important modulatory role upon metabolic homeostasis by affecting energy handling and producing several bioactive molecules that regulate insulin sensitivity, as well as immune and vascular responses [4]. On the other hand, chronic administration of excess nutrients expands AT, inducing a simultaneous change in its cellular and matrix remodelling [5], as well as marked metabolic and endocrine dysfunctions, as in the case of obesity.

Regarding the FRD, the increase in VAT mass and the associated dysfunction depends on a hypertrophy (i.e. the unhealthy expansion) of its cells [6] and an increased peripheral/VAT oxidative stress [3]. However, the underlying mechanism whereby the FRD induces this selective adipocyte hypertrophy rather than its hyperplasia remains unknown.

Adipogenesis is a multistep process that is regulated by several transcription factors and hormones, whereby the precursor cells (pre-adipocytes) differentiate into mature adipocytes [7]. In this process, committed pre-adipocytes present in the stromal vascular fraction (SVF) of the AT pad express the transcriptional regulator of pre-adipocyte determination, Zfp423 [8]. This signal in turn activates the basal expression of pre-adipocyte peroxisome proliferator-activated receptor (PPAR)-γ2 [8], a key pro-adipogenic signal [9,10] that assures pre-adipocyte differentiation. Complementarily, extracellular factors, such as insulin [11], glucocorticoids [11] and LEP [12], also stimulate pre-adipocyte differentiation.

On the other hand, pre-adipocyte factor-1 (Pref-1), a transmembrane protein specifically produced by pre-adipocytes, exerts the most potent inhibitory signal of the adipogenic process [13–15]. Its expression decreases progressively in cells undergoing differentiation, becoming undetectable in mature adipocytes [14]. The wingless-type MMTV (Wnt) family of secreted signalling proteins also plays a negative modulatory role in adipocyte differentiation process [16]. Indeed, activation of Wnt signalling by Wnt-10b inhibits the differentiation of pre-adipocytes *in vitro*. Furthermore, mice with Wnt-10b over expression showed a 50% decrease in total body fat [17,18]. These animals are also resistant to AT accumulation when fed a high-fat diet, as well as being more glucose-tolerant and insulin-sensitive than wild-type mice.

Although increased fatness and different endocrine and metabolic alterations have been identified in the human metabolic syndrome, as far as we are aware, the effect of FRD intake on the adipogenic capacity of VAT precursor cells has not been addressed. We assumed that changes in the pre-adipocyte maturation process could play an important role in the development of this dysfunctional hypertrophic state. Thus, testing this hypothesis would not only provide new knowledge on the pathogenesis of VAT cell hypertrophy, but also present an opportunity to implement preventive strategies at an early stage of its development. Accordingly, in the present study, we investigated *in vitro* the overall adipogenic capacity of VAT precursor cells isolated from FRD-fed rats.

Results

Food intake, body weight and metabolic parameters in the SVF cell donor

A comparable 21-day mean intake of total food energy was recorded in both groups of rats (212.3 ± 14.3 kj·rat^{-1}·day^{-1} and 232.6 ± 18.9 kj·rat^{-1}·day^{-1} in commercial diet (CD) and FRD rats, respectively; $P > 0.05$, $n = 14/16$ rats per group).

Although the intake of an FRD did not induce significant changes in body weight after the 3-week study period, it induced a significant increase in VAT mass and adipocyte size ($P < 0.05$) (Table 1). However, no significant differences between groups were found in the number of SVF cells·g^{-1} isolated from VAT (Table 1).

The administration of an FRD to rats did not modify plasma glucose and corticosterone levels, although these animals had higher peripheral levels of insulin, triglyceride, LEP and thiobarbituric acid reactive substances (TBARS) ($P < 0.05$ compared to CD) (Table 1).

Table 1. Rat anthropometry and circulating levels of metabolic parameters. Body weight, VAT pad weight, VAT SVF cell number and plasma levels of several parameters in CD- and FRD-fed rats. Values represent the mean ± SEM ($n = 8$ rats per group).

	CD	FRD
Body weight (g)	368 ± 13	388 ± 12
VAT mass (g)	3.28 ± 0.27	4.27 ± 0.21*
VAT adipocyte size (μm)	49.1 ± 2.2	58.3 ± 1.8*
VAT SVF cell number/g VAT (x 10^5)	2.95 ± 0.46	2.58 ± 0.25
Glucose (mM)	6.17 ± 0.21	6.34 ± 0.14
Insulin (ng·mL^{-1})	1.57 ± 0.18	2.27 ± 0.15*
Triacylglycerol (mM)	0.91 ± 0.06	1.69 ± 0.11*
LEP (ng·mL^{-1})	2.51 ± 0.24	3.45 ± 0.31*
Corticosterone (μg·dL^{-1})	10.55 ± 2.76	11.03 ± 2.46
TBARS (pmol·mg protein^{-1}·mL^{-1})	57.98 ± 5.85	74.11 ± 4.76*

*$P < 0.05$ compared to CD.

In vitro proliferation capacity of VAT SVF cells

The proliferation capacity of SVF cells, measured as the number of cultured cells counted at a 24-h interval between proliferation days (Pd) 1 and 9, showed no significant differences between cells isolated from either CD or FRD rats (i.e. the slopes of the proliferation curves were 22 089 ± 1117 cells·24 h^{-1} and 20 106 ± 1205 cells·24 h^{-1} in CD and FRD, respectively (n = 3–4 different experiments, with four wells per group per experimental day; $P > 0.05$).

In vitro VAT SVF cell differentiation: impact of FRD feeding

Accumulation of cytoplasmic lipid, a classical marker of adipocyte differentiation [9], was already detected on differentiation day (Dd) 2 and thereafter in both groups (Fig. 1, upper left). Despite the cellular lipid content (quantified by Oil-Red O staining) being similar in both groups on Dd 2, it became significantly higher in FRD on Dd 4 and thereafter ($P < 0.05$) (Fig. 1, upper left).

Because LEP is an adipokine synthesized by adipocytes but not by precursor cells, its presence/release also represents a reasonable marker of cell differentiation. Although the LEP concentration in the culture medium was negligible on Dd 2 in both cell groups, it became detectable on Dd 4 and showed a significant time-dependent increase from Dd 6 to Dd 10 in cells obtained from FRD animals ($P < 0.05$ versus respective CD values) (Fig. 1, lower panel). This differential pattern of adipokine production fully agrees with the one recorded in cell lipid appearance throughout the culture period.

Complementary, at the end of the differentiation period (Dd 10), the cell expression levels of marker genes of fully differentiated adipocytes, adiponectin (ADIPOQ) and LEP, as well as the intracellular insulin mediator insulin receptor substrate-1 (IRS-1), were significantly higher in cells obtained from FRD than

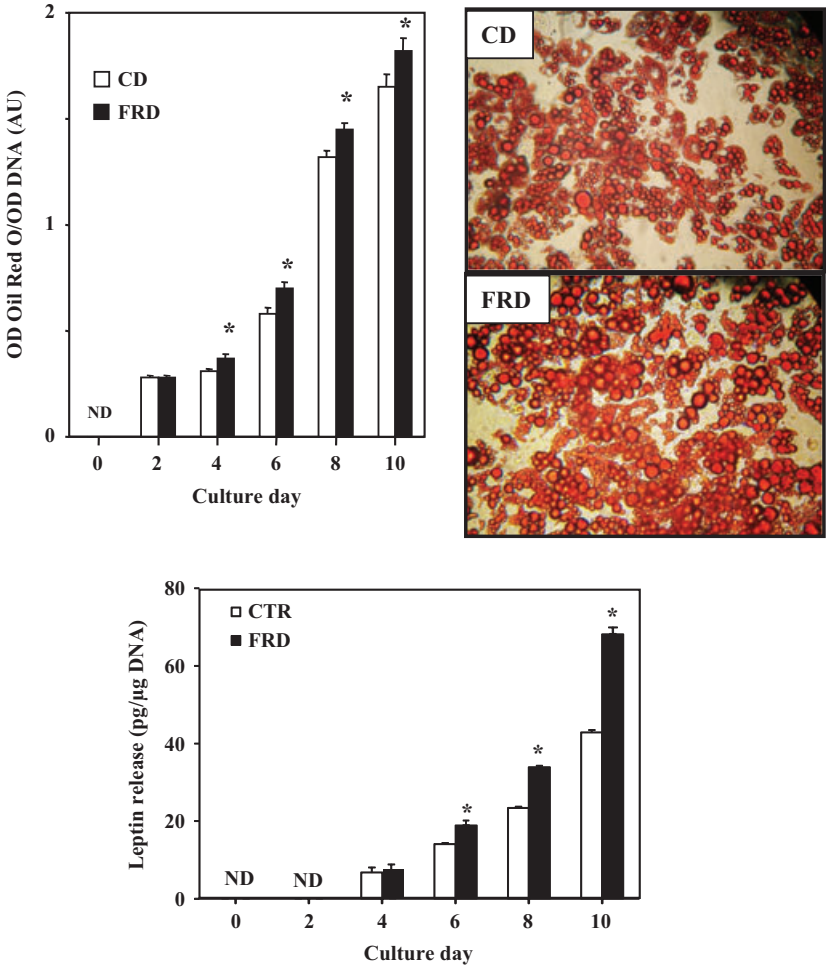

Fig. 1. Time-dependent accumulation of intracellular lipids during *in vitro* differentiation of SVF cells isolated from VAT of CD and FRD rats (upper left). Representative micrographs of *in vitro* fully differentiated cells (Dd 10) in CD and FRD after staining with Oil-Red O (upper right). Time-dependent LEP secretion into the culture medium by isolated VAT SVF cells (CD and FRD) undergoing *in vitro* differentiation (lower). Values are the mean ± SEM (n = 4/5 different experiments with 10/12 wells per day per experiment). •$P < 0.05$ compared to CD.

CD rats ($P < 0.05$) (Fig. 2). However, no significant group difference was recorded in the cell concentration of PPAR-γ2 mRNA [1.01 ± 0.18 arbitrary units (AU) and 1.19 ± 0.32 AU in CD and FRD, respectively; $P > 0.05$].

FRD-induced changes upon adipocyte maturation rate

Quantitative assessment of the number of cells showing lipidic vacuoles on Dd 10 (performed in cover-slip fixed cells) showed comparable percentage values of mature adipocytes (60.2 ± 4.24% and 57.7 ± 4.93%, respectively; $n = 4/5$ different experiments). However, we found variable differences between groups throughout the whole maturation process: comparable values at stage I (Fig. 3, lower), a significantly lower percentage in FRD cells at stage II and a larger one at stage III ($P < 0.05$ versus CD) (Fig. 3, lower).

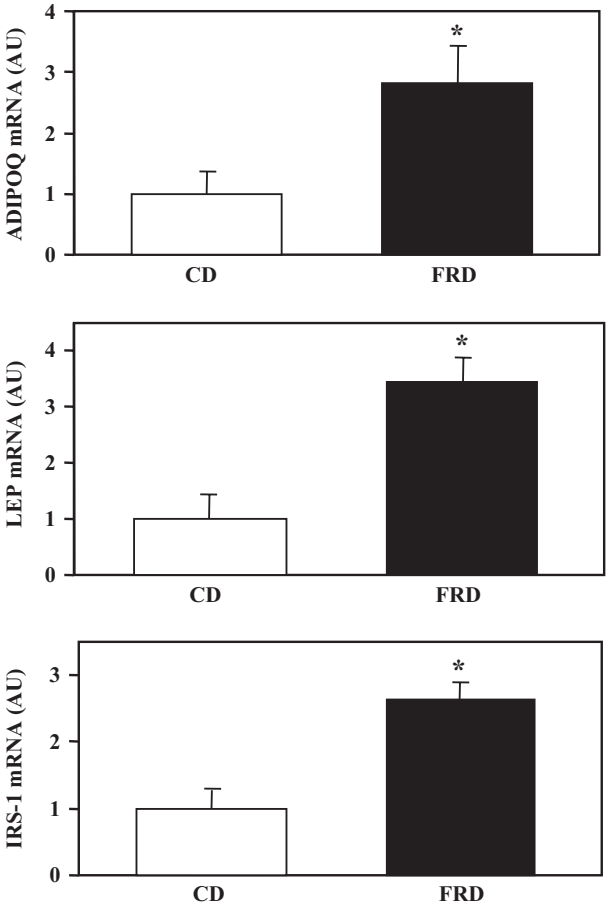

Fig. 2. mRNA concentrations of adipogenesis markers: ADIPOQ (upper), LEP (middle) and IRS-1 (lower), measured in fully *in vitro* differentiated adipocytes (Dd 10) isolated from CD and FRD animals. Values are expressed in AU (arbitrary units) and in relation to values of the corresponding marker displayed by CD SVF cells. Results are the mean ± SEM ($n = 4/5$ different experiments with 10/12 wells per experiment). $^{\bullet}P < 0.05$ compared to CD.

Analysis of VAT precursor cells by flow cytometry

VAT SVF cells were analyzed by flow cytometry using the strategy of cell identification as noted below. The ratio $CD34^{+}/CD45^{-}/CD31^{-}$ over the total SVF cell number was similar in both groups (7.77 ± 1.35% and 8.51 ± 0.81% in CD and FRD cells, respectively; $n = 4$ independent experiments). A representative dot plot of VAT progenitor cells from both experimental groups is depicted in Fig. 4.

VAT SVF cell commitment and adipogenic signals

Zpf423 and PPAR-γ2, two markers of the degree of differentiation commitment of adipocyte precursors, showed a significantly higher expression in VAT SVF cells isolated from FRD animals ($P < 0.05$) (Fig. 5A, B). Conversely, cell mRNA concentrations of mineralocorticoid receptor (MR) and glucocorticoid receptor (GR), two pro-adipogenic signal transducers, showed comparable values in both groups (CD versus FRD; MR: 1.03 ± 0.18 AU versus 0.93 ± 0.13 AU; $n = 5/6$ different experiments; GR: 1.01 ± 0.14 AU versus 0.92 ± 0.17 AU; $n = 5/6$ different experiments). On the other hand, mRNA concentrations of anti-adipogenic factors Pref-1 and Wnt-10b were significantly lower in FRD than in CD VAT SVF cells ($P < 0.05$) (Fig. 5C,D).

Discussion

We have previously shown that administration of an FRD to normal male rats for 3 weeks induces several VAT alterations, such as an increase in VAT mass and adipocyte size, changes in its lipid composition, and a marked increase in the release of fatty acids and pro-inflammatory adipokines [1]. Based on these data and other reports in the literature [19–22], we assumed that adipocyte hypertrophy was responsible, at least partly, for this multiple VAT expansion/dysfunction. Thus far, however, there is no reported evidence on the potential effect of FRD administration upon *in vitro* adipogenesis. In this regard, the present study clearly shows that the effect of the FRD starts early at the stage of SVF precursor cells, increasing the expression of pro-adipogenic gene factors and decreasing that of anti-adipogenic ones.

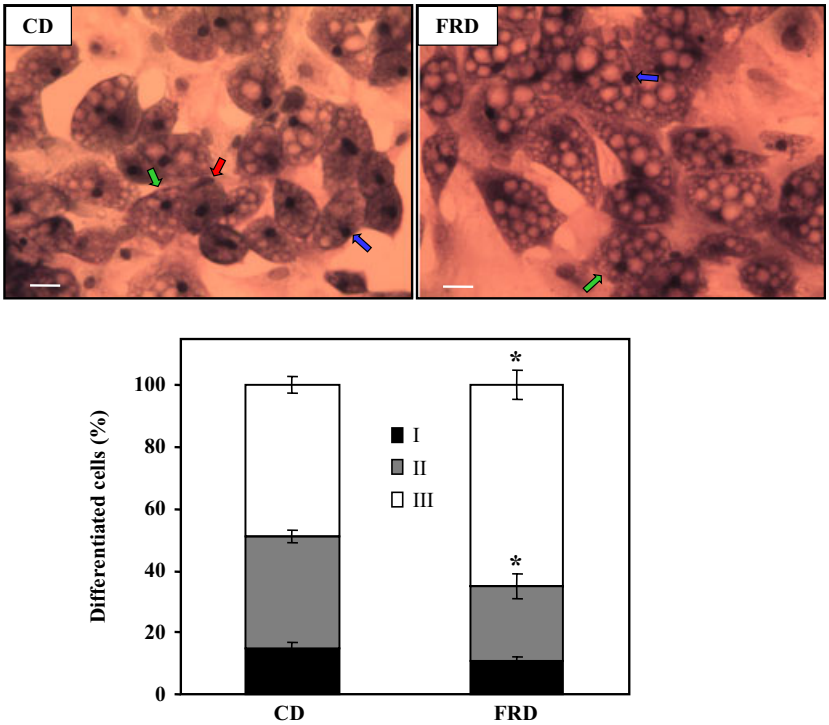

Fig. 3. Representative fields containing fully *in vitro* differentiated adipocytes (Dd 10) from CD (upper left) and FRD (upper right) rats, displaying different degrees of maturation according to the nucleus position: I, central (red arrows); II, center (green arrows); III, fully peripheral (blue arrows) (white bars = 200 μm). The percentage of fully *in vitro* differentiated adipocytes from CD and FRD according to their maturation degree is also shown (lower panel). Values are the mean ± SEM (n = 4/5 different experiments; data from 200/250 cells were recorded in each experiment). •$P < 0.05$ compared to CD values.

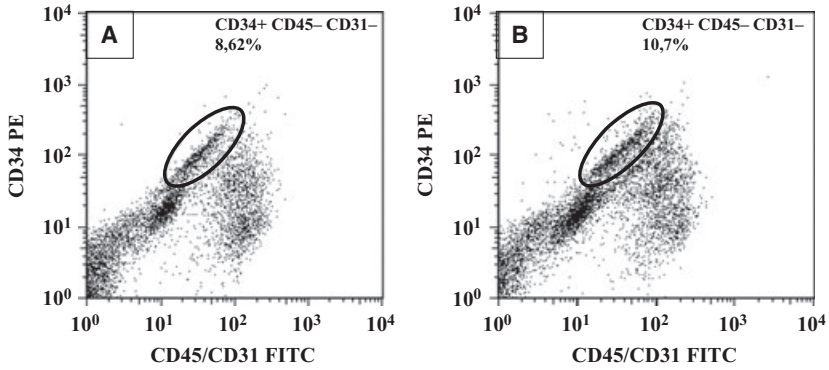

Fig. 4. Representative dot plots showing the staining profile of SVF cells isolated from VAT pads of (A) CD and (B) FRD rats. Representative $CD34^+CD45^-CD31^-$ gates used are indicated (black ellipses). FITC, fluorescein isothiocyanate.

AT mass expansion is the result of the balance between enlarged cell size (hypertrophy) and increased cell number (hyperplasia). Although adipocyte volume/size mainly reflects energy (lipid) and adipokine storage, their numbers are the main indicator of adipocyte renewal. In the present study, there was no difference in both the number and proliferation capacity of VAT precursor SVF cells measured in the CD and FRD groups; these data suggest that the increased adipogenic capacity recorded could be the result of a real different maturation capacity rather than changes in the number of precursors in the FRD group. This assumption is strongly supported by (a) a higher expression of pro-adipogenic factors and a lower expression of anti-adipogenic ones in precursor cells isolated from FRD rats; (b) an enhanced, time-dependent appearance of adipogenic markers, such as cell lipid content and adipokine expression (ADIPOQ and LEP), as well as LEP release; and (c) a larger percentage of fully differentiated cells (nucleus position, either close or adjacent to the cell membrane).

It is known that Zpf423 is a signal that regulates preadipocyte commitment and, subsequently, PPAR-γ2 expression [8]. Additionally, Zfp423 acts as a co-activator of Smad proteins and amplifies the pro-adipogenic and PPAR- γ2-inducing actions of bone morphogenetic protein signalling [8,23]. Moreover, silencing Zpf423 expression induces a drastic reduction in PPAR-positive cell number [8]. In this regard, our data show that, despite the comparable number of

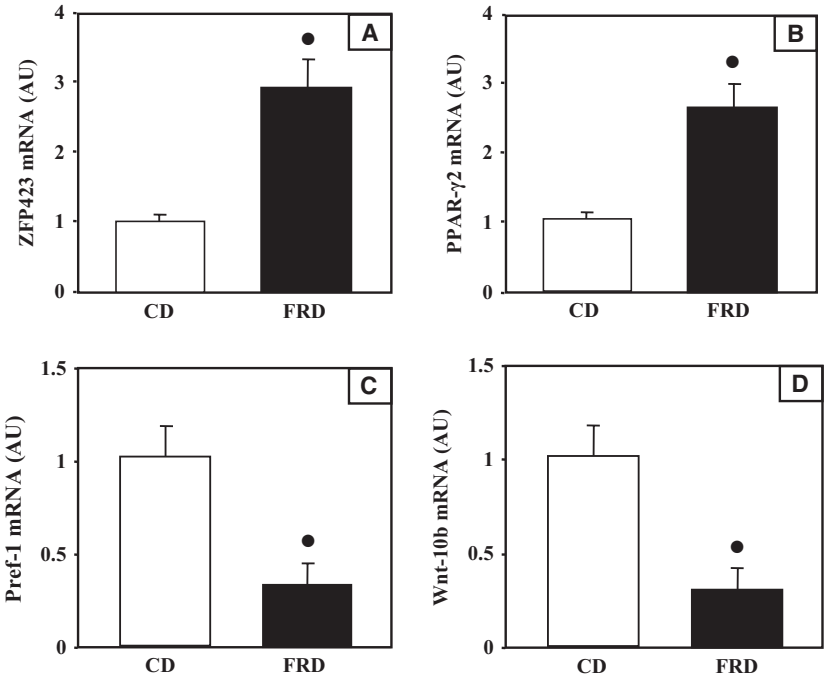

Fig. 5. mRNA concentrations of pro-adipogenic (ZFP423, A; PPAR-γ2, B) and anti-adipogenic (Pref-1, C; Wnt-10b, D) factors in SVF cells freshly isolated from CD and FRD VAT. Data are expressed in arbitrary units (AU) and in relation to values of the corresponding marker displayed by CD SVF cells. Values are the mean ± SEM (n = 5/6 different experiments). $^{\bullet}P < 0.05$ compared to CD.

VAT precursors ($CD34^+/CD45^-/CD31^-$) isolated from CD and FRD rats, those cells isolated from the latter rats over-expressed Zpf423 and PPAR-γ2, thus demonstrating a larger proportion of cells already committed to promptly differentiate into adipocytes [8]. Conversely, the expression of two potent anti-adipogenic factors, Pref-1 and Wnt-10b [24], was significantly lower in these cells. These data suggest that the overall higher adipogenic capacity measured in SVF cells isolated from FRD VAT results, at least partly, from the combination of an uneven expression of pro-adipogenic factors/genes (enhanced) and those exerting a negative (decreased) modulatory effect. These changes *in vivo* would apparently remain constant during the *in vitro* culture, being responsible for the uneven differentiation velocity recorded between groups.

We still do not know the precise mechanism that triggers this pro-/anti-adipogenic balance in FRD rats. It is tempting to speculate that the general oxidative stress (TBARS) and local oxidative stress (VAT) [3] present in FRD animals could be one such trigger. This state of FRD-induced high oxidative stress could in turn decrease sirtuin-1 production [25], a NAD^+-dependent histone deacetylase that represses PPARγ expression [26] and thus inhibits adipogenesis. Therefore, diminished cell sirtuin-1 production would increase PPARγ production, thus triggering adipogenesis. Moreover, high PPARγ signalling is able to stimulate another pro-adipogenic factor, Setd8, a histone methyltransferase [27], once again epigenetically potentiating an early adipogenic process. Such potential epigenetic changes would contribute to the establishment and maintenance of progenitor cell determination in culture. Epigenetic mechanisms might explain why the characteristic of progenitors of different AT depots are retained *in vitro* for several generations outside of organism environment. However, it cannot be ruled out that other mechanisms may contribute to the persistence of the expression pattern of progenitors cells isolated from FRD rats [28]. On account of the results of the present study, studies are in progress in our laboratories aiming to test this hypothesis.

In summary, the data obtained in the present study indicate that VAT precursor cells isolated from normal rats fed an FRD display an increased adipogenic capacity under *in vitro* conditions. Changes in the lipid content of VAT precursor cells were the earliest marker of this process. Such an effect would result from a breakdown of the balance between the pro- and anti-adipogenic circulating and tissue modulators that switch the balance in favour of the former. FRD rats showed an increase in insulin plasma levels and in the VAT expression of its intracellular mediator (IRS-1), as well as in the percentage of precursor cell commitment, together with a decrease in the VAT SVF cell expression of key anti-adipogenic factors. The cellular changes described would be sufficient to settle the faster adipogenic process reported in the present study. We could assume that the VAT mass expansion observed shortly after administration

of an FRD to normal rats depends on the combination of an initial accelerated adipogenic process and a final cell size enlargement. It remains to be confirmed whether both processes perpetuate in the case of longer FRD administration, or whether only cell hypertrophy remains responsible for the potential additional VAT mass expansion, as occurs in advanced/morbid obesity [1,2,29,30]. Regardless of the answer to this question, our data show that the FRD effect starts very early in the adipogenic process. From a clinical point of view, the implementation of preventive strategies at that stage could probably be more effective than those applied later, when the abnormality is fully developed.

Materials and methods

Animals and treatment

As described previously [1–3], normal adult male Sprague–Dawley rats (aged 60 days) were kept in a temperature-controlled environment under a 12 : 12 h light/dark cycle at at 23 ºC. Animals were fed a Purina (Ganave SA, Pilar, Argentina) commercial rat chow *ad libitum* for 3 weeks and either tap water only (conventionally designated as the CD) or with the addition of 10% fructose (w/v) in drinking water (conventionally designated as the FRD). CD and FRD rats were then decapitated in nonfasting conditions (between 08.00 h and 09.00 h) and trunk blood was collected into EDTA-coated tubes. Tubes were rapidly centrifuged at 2500 ***g*** for 15 min at 4 °C, and plasma samples were kept frozen at −80 °C until metabolite measurements. VAT was aseptically dissected, weighed and placed in sterile Petri dishes containing 10 mL of sterile DMEM-low glucose (LG) (1 $g \cdot L^{-1}$). Animals were sacrificed in accordance with protocols for animal use, in agreement with NIH guidelines for the care and use of experimental animals. All experiments received approval from our Institutional Animal Care Committee.

Peripheral parameter measurements

Plasma levels of LEP [31], insulin [32] and corticosterone [33] were determined by a specific radioimmunoassay previously developed in our laboratory. Circulating glucose (Wiener Laboratory, Rosario, Argentina) and triglyceride (Wiener Laboratory, Rosario, Argentina) levels were measured using commercial kits. Plasma lipid peroxidation was determined by measuring TBARS, as calculated by the extinction coefficient for the malondialdehyde-thiobarbituric acid reaction complex of 1.56×10^5 $M \cdot cm^{-1}$, and expressed as pmol malondialdehyde·mg plasma $protein^{-1}$, as measured with the Bio-Rad Protein Assay kit (Bio-Rad Lab, Hercules, CA, USA) [3].

Histological studies

VAT pads were removed and immediately fixed in 4% paraformaldehyde (in 0.2 M phosphate buffer) at 4 °C for a maximum of 3 days. Tissues were then washed with 0.01 M $NaCl/P_i$ and immersed in 70% ethanol for 24 h before being processed and embedded in paraffin. Sections of 4 μm were obtained at different levels of the blocks, stained with haematoxylin and eosin, and then examined with a Jenamed 2 light microscope (Carl Zeiss, Oberkochen, Germany). Quantitative morphometric analysis was performed using a RGB charge-coupled device camera (Sony Corp., Tokyo, Japan) together with OPTIMAS software (Bioscan Incorporated, Edmons, WA, USA) (× 40 objective). For each VAT sample, one section and three levels were selected ($n = 3$ animals per group). Systematic random sampling was used to select ten fields for each section and a minimum of 100 cells per group were examined. We then measured adipocyte number and diameter [1].

VAT SVF cell isolation

Fresh VAT pads from CD and FRD rats were digested with collagenase as described previously [34]. Briefly, VAT pads were minced and digested with 1 $mg \cdot mL^{-1}$ collagenase solution in DMEM-LG for 1 h at 37 ºC. After centrifugation at 750 ***g*** for 15 min, floating mature adipocytes were discarded and the SVF cell pellet was collected, filtered in a 50-μm mesh nylon cloth, and washed twice with DMEM-LG.

Proliferation assay

VAT SVF cells from both groups where seeded at a density of 15 000 $cells \cdot well^{-1}$ in sterile 24-well plates (Greiner Bio-One GmbH, Frickenhausen, Germany) and cultured at 37 °C in a 5% CO_2-atmosphere in DMEM-LG supplemented with 20 nM Hepes, 10% fetal bovine serum (v/v), 100 $U \cdot mL^{-1}$ penicillin and 100 $U \cdot mL^{-1}$ streptomycin [34]. Every 24 h, cells (four wells per day) were washed (× 1) with $NaCl/P_i$ buffer. Thereafter, a 0.25% (w/v) trypsin solution dissolved in $NaCl/P_i$-EDTA was added for 2–3 min at 37 °C; the cell suspension was then collected and cell number was determined in a Newbauer chamber. This procedure was performed every 24 h between days Pd 1 and Pd 9 of culture.

Precursor cell differentiation assay

In separate experiments, after proliferating CD and FRD SVF cells reached 65–5% confluence on Pd 5–6, they were induced to differentiate (differentiation day zero, Dd 0) by addition of a classical mix solution: 5 $\mu g \cdot mL^{-1}$ insulin, 0.25 μM dexamethasone, 0.5 mM 3-isobutyl-L-methylxanthine in DMEM-LG-Hepes, supplemented with 10% fetal

bovine serum and antibiotics [34]. After 48 h, media were removed and replaced by fresh media containing insulin (5 μg·mL^{-1}), fetal bovine serum (10%) and antibiotics, and then cultured for 10 days (Dd 10). Through this period, media were replaced by fresh media every 48 h. After replacement, medium samples were kept frozen at −20 °C until measurement of LEP concentrations (see below). Cell samples were processed on different Dds for several determinations, as described below.

Leptin release

LEP concentration in the medium was determined by a specific radioimmunoassay [31]. In this assay, the standard curve ranged between 50 and 12 500 pg·mL^{-1} (intra- and inter-assay coefficients of variation of 4–6% and 5–8%, respectively).

Lipid cell content (Oil-Red O staining)

Cells from Dd 0 through Dd 10 were washed with NaCl/P_i and fixed with 10% formalin in NaCl/P_i for 10–15 min. Then cells were quickly washed with 60% isopropanol and stained for 1 h with Oil-Red O solution (2 : 3 v/v H_2O : isopropanol, containing 0.5% Oil-Red O) [35]. After staining, the cells were washed three times with NaCl/P_i and the dye from stained material was extracted by adding 200 μL of isopropanol for 10 min. To quantify cell lipid content, D_{510} was measured in a spectrophotometer. The remaining cells were digested with 200 μL of 0.25% Trypsin solution in NaCl/P_i-EDTA at 37 °C for 24 h. Subsequently, the cell suspension was centrifuged at 8000 ***g*** for 15 s and D_{260} of the supernatants was measured for DNA quantification. Cell lipid content (as measured by Oil-Red O) was then expressed as a function of the corresponding cell DNA content.

RNA isolation and real-time quantitative PCR

Total RNA was isolated from cells of both groups by the single-step, acid guanidinium isothiocyanate–phenol–chloroform extraction method (Trizol; Invitrogen, Life Technologies, Carlsbad, CA, USA; catalogue number 15596-026) [36]. In total, 1 μg of total RNA was reverse transcribed using random primers (250 ng) and Superscript III Rnase HReverse Transcriptase (200 units/μL^{-1} Invitrogen Life Technologies; catalogue number 18989-093). The primers applied were β-actin (ACTB), ADIPOQ, GR, IRS-1, LEP, MR, PPAR-γ2, Pref-1 and Wnt-10b (Table 2). In total, 2 μL of the reverse transcription mix was amplified using the QuantiTect Syber Green PCR kit (Qiagen, Valencia, CA, USA; catalogue number 204143), adding 0.5 μM of each specific primer, and then measured with a LightCycler Detection System (MJ Mini Opticon; Bio-Rad). PCR efficiency was near 1. The threshold cycle (Ct) was measured in separate tubes in duplicate. The identity and purity of the amplified product were checked by electrophoresis on agarose mini-gels, and analysis of the melting curve was carried out at the end of amplification. Differences between Ct were calculated in every sample for each gene of interest: Ct gene of interest – Ct reporter gene ACTB whose mRNA levels did not differ between the control and test groups. Relative changes in the expression level of one specific gene (ΔΔCt) were calculated as the ΔCt of the test group minus the ΔCt of the control group, and then presented as $2^{-\Delta\Delta Ct}$.

Table 2. Primers designed for a high homology region of different genes and used for real time RT-PCR analyses. GBAN, GenBank Accession Number. Amplicon length is given in bp.

Gene	Primers	GBAN	bp
ACTB	se, 5′-AGCCATGTACGTAGCCATCC-3′ as, 5′-ACCCTCATAGATGGGCACAG-3′	NM_031144	115
ADIPOQ	se, 5′-AATCCTGCCCAGTCATGAAG-3′ as, 5′-TCTCCAGGAGTGCCATCTCT-3′	NM_144744	159
GR	se, 5′-TGCCCAGCATGCCGCTATCG-3′ as, 5′-GGGGTGAGCTGTGGTAATGCTGC-3′	NW_047512	170
LEP	se, 5′-GAGACCTCCTCCATCTGCTG-3′ as, 5′-CTCAGCATTCAGGGCTAAGG-3′	NM_013076	192
MR	se, 5′-TCGCTCCGACCAAGGAGCCA-3′ as, 5′-TTCGCTGCCAGGCGGTTGAG-3′	NM_013131	193
PPAR-γ2	se, 5′-AGGGGCCTGGACCTCTGCTG-3′ as, 5′-TCCGAAGTTGGTGGGCCAGA-3′	NW_047696	185
Pref-1	se, 5′-TGCTCCTGCTGGCTTTCGGC-3′ as, 5′-CCAGCCAGGCTCACACCTGC-3′	NM_053744	113
Wnt-10b	se, 5′-AGGGGCTGCACATCGCCGTTC-3′ as, 5′-ACTGCGTGCATGACACCAGCAG-3′	NW_047784	175
Zfp423	se, 5′-CCGCGATCGGTGAAAGTTG-3′ as, 5′-CACGGCTGGATTTCCGATCA-3′	NM_053583.2	121

Cell differentiation and maturation

Additionally, 65–75% confluent VAT SVF cells seeded on sterile cover-glasses were differentiated on Pd 5–6 as described above. On Dd 10, cells were fixed with 10% formalin solution for 1 h at room temperature, and then stained with haematoxylin and eosyn. The percentage of differentiated cells was calculated by counting the total number of cells and the number of cells containing lipid droplets when visualized under a light microscope ($n = 4/5$ different experiments, counting, 40–50 cells per field from five different fields per experiment, thus summing 200–250 cells counted per experiment, × 40 magnification). Lipid-containing cells were assigned to three graded stages of maturation according to the position of the nucleus [37]: stage I (central nucleus position); stage II (between center and peripheral nucleus position); and stage III (fully peripheral nucleus position). The percentage of cells corresponding to the different maturation stages was then expressed in relation to the total number of differentiated cells. Image analysis was assessed using a light microscope and analysis IMAGE software (IMAGE PROPLUS, version 5.0; Media Cybernetics, Inc., Bethesda, MD, USA).

Flow cytometry analysis

Experiments were performed using a FACSCalibur flow cytometer (Becton-Dickinson Biosciences, Franklin Lakes, NJ, USA). Briefly, SVF cells from VAT pads of CD and FRD animals were isolated and at least 2×10^5 cells (in 100 μL of NaCl/P_i–0.5% BSA) were incubated with fluorescent antibodies or the respective isotype controls (1 : 50 dilution, 1 h at 4 ºC). After washing, flow cytometry analysis was performed. Total SVF cells were initially identified by size and complexity on the basis of forward scatter and side scatter. Using a combination of surface cell markers, CD34 (expressed on haematopoietic stem and progenitor cells), CD31 (expressed on leukocytes and endothelial cells) and CD45 (expressed on hematopoietic cells), VAT progenitor cells were then identified as: $CD34^+/CD45^-/CD31^-$ cells [38]. Conjugated monoclonal antibodies used for flow cytometry analyses were anti-rat CD34:phycoerythrin (Santa Cruz Biotechnology Inc, Santa Cruz, CA, USA), anti-rat CD45:fluorescein isothiocyanate (Santa Cruz Biotechnology Inc) and anti-rat CD31:fluorescein isothiocyanate (Santa Cruz Biotechnology Inc). Samples were analyzed using the CELLQUEST PRO (Becton-Dickinson Biosciences) and FLOWJO (Tree Star Inc., Ashland, OR, USA).

Statistical analysis

Data were analyzed by analysis of variance (one- or two-way) followed by Fisher's test. A nonparametric Mann–Whitney test was applied in the analysis of values from cell mRNA expression. Morphometric data were analyzed by the least significant difference test [39]. Results are expressed as the mean ± SEM. $P < 0.05$ was considered statistically significant.

Acknowledgements

The present study was supported by grants received from the Consejo Nacional de Investigaciones Científicas y Técnicas (CONICET) (PIP 2009-0704 to E.S. and 2009-5020 to J.J.G); Fondation pour la Recherche en Endocrinologie, Diabetologie et Metabolisme (Suisse; 2012/2014 to E.S.); and Fondo para la Investigación Científica y Tecnológica (FONCyT) (PICT 2001-1051 to E.S.). A.G., E.S. G.M. and J.J.G. are members of the Research Career of CONICET. M.G.Z. and J.P.F. are fellows of CONICET and Universidad Nacional de La Plata, Argentina, respectively. The authors gratefully thank D. Castrogiovanni and A. Díaz for their excellent technical assistance, as well as A. Di Maggio for careful correction and editing of the manuscript.

References

1 Alzamendi A, Giovambattista A, Raschia A, Madrid V, Gaillard RC, Rebolledo O, Gagliardino JJ & Spinedi E (2009) Fructose-rich diet-induced abdominal adipose tissue endocrine dysfunction in normal male rats. *Endocrine* **35**, 227–232.

2 Alzamendi A, Giovambattista A, García ME, Rebolledo OR, Gagliardino JJ & Spinedi E (2012) Effect of pioglitazone on the fructose-induced abdominal adipose tissue dysfunction. *PPAR Res* **2012**, 259093. doi:10.1155/2012/259093

3 Fariña JP, García ME, Alzamendi A, Giovambattista A, Marra CA, Spinedi E & Gagliardino JJ (2013) Antioxidant treatment prevents the development of fructose-induced abdominal adipose tissue dysfunction. *Clin Sci (Lond)* **125**, 87–97.

4 Adamczak M & Wiecek A (2013) The adipose tissue as an endocrine organ. *Semin Nephrol* **33**, 2–13.

5 Huang G & Greenspan DS (2012) ECM roles in the function of metabolic tissues. *Trends Endocrinol Metab* **23**, 16–22.

6 Alzamendi A, Castrogiovanni D, Ortega HH, Gaillard RC, Giovambattista A & Spinedi E (2010) Parametrial adipose tissue and metabolic dysfunctions induced by fructose-rich diet in normal and neonatal-androgenized adult female rats. *Obesity (Silver Spring)* **18**, 441–448.

7 Armani A, Mammi C, Marzolla V, Calanchini M, Antelmi A, Rosano GM, Fabbri A & Caprio M (2010) Cellular models for understanding adipogenesis, adipose dysfunction, and obesity. *J Cell Biochem* **110**, 564–572.

8 Gupta RK, Arany Z, Seale P, Mepani RJ, Ye L, Conroe HM, Roby YA, Kulaga H, Reed RR & Spiegelman BM (2010) Transcriptional control of preadipocyte determination by Zfp423. *Nature* **25** (464), 619–623.
9 Mandrup S & Lane MD (1997) Regulating adipogenesis. *J Biol Chem* **272**, 5367–5370.
10 Tontonoz P & Spiegelman BM (2008) Fat and beyond: the diverse biology of PPARgamma. *Annu Rev Biochem* **77**, 289–312.
11 Gregoire FM, Smas CM & Sul HS (1998) Understanding adipocyte differentiation. *Physiol Rev* **78**, 783–809.
12 Machinal-Quélin F, Dieudonné MN, Leneveu MC, Pecquery R & Giudicelli Y (2002) Proadipogenic effect of leptin on rat preadipocytes in vitro: activation of MAPK and STAT3 signaling pathways. *Am J Physiol Cell Physiol* **282**, C853–C863.
13 Jing K, Heo JY, Song KS, Seo KS, Park JH, Kim JS, Jung YJ, Jo DY, Kweon GR, Yoon WH *et al.* (2009) Expression, regulation and function of Pref-1 during adipogenesis of human mesenchymal stem cells (MSCs). *Biochim Biophys Acta* **1791**, 816–826.
14 Smas CM & Sul HS (1993) Pref-1, a protein containing EGF-like repeats, inhibits adipocyte differentiation. *Cell* **73**, 725–734.
15 Sul HS (2009) Minireview: Pref-1: role in adipogenesis and mesenchymal cell fate. *Mol Endocrinol* **23**, 1717–1725.
16 Bennett CN, Ross SE, Longo KA, Bajnok L, Hemati N, Johnson KW, Harrison SD & MacDougald OA (2002) Regulation of Wnt signaling during adipogenesis. *J Biol Chem* **277**, 30998–31004.
17 Longo KA, Wright WS, Kang S, Gerin I, Chiang S-H, Lucas PC, Opp MR & MacDougald OA (2004) Wnt10b inhibits development of white and brown adipose tissues. *J Biol Chem* **279**, 35503–35509.
18 Kang S, Bajnok L, Longo KA, Petersen RK, Hansen JB, Kristiansen K & MacDougald OA (2005) Effects of Wnt signaling on brown adipocyte differentiation and metabolism mediated by PGC-1 alpha. *Mol Cell Biol* **25**, 1272–1282.
19 Dekker MJ, Su Q, Baker C, Rutledge AC & Adeli K (2010) Fructose: a highly lipogenic nutrient implicated in insulin resistance, hepatic steatosis, and the metabolic syndrome. *Am J Physiol Endocrinol Metab* **299**, E685–E694.
20 Johnson RJ, Segal MS, Sautin Y, Nakagawa T, Feig DI, Kang DH, Gersch MS, Benner S & Sánchez-Lozada LG (2007) Potential role of sugar (fructose) in the epidemic of hypertension, obesity and the, metabolic syndrome, diabetes, kidney disease, and cardiovascular disease. *Am J Clin Nutr* **86**, 899–906.
21 Huang B-W, Chiang M-T, Yao H-T & Chiang W (2004) The effect of high-fat and high-fructose diets on glucose tolerance and plasma lipid and leptin levels in rats. *Diabetes Obes Metab* **6**, 120–126.
22 Lundgren M, Svensson M, Lindmark S, Renström F, Ruge T & Eriksson JW (2007) Fat cell enlargement is an independent marker of insulin resistance and 'hyperleptinaemia'. *Diabetologia* **50**, 625–633.
23 Hata A, Seoane J, Lagna G, Montalvo E, Hemmati-Brivanlou A & Massagué J (2000) OAZ uses distinct DNA- and protein-binding zinc fingers in separate BMP-Smad and Olf signaling pathways. *Cell* **100**, 229–240.
24 Wang Y, Hudak C & Sul HS (2010) Role of preadipocyte factor 1 in adipocyte differentiation. *Clin Lipidol* **5**, 109–115.
25 Akar F, Uludağ O, Aydın A, Aytekin YA, Elbeg S, Tuzcu M & Sahin K (2012) High-fructose corn syrup causes vascular dysfunction associated with metabolic disturbance in rats: protective effect of resveratrol. *Food Chem Toxicol* **50**, 2135–2141.
26 Picard F, Kurtev M, Chung N, Topark-Ngarm A, Senawong T, Machado De Oliveira R, Leid M, McBurney MW & Guarente L (2004) Sirt1 promotes fat mobilization in white adipocytes by repressing PPAR-gamma. *Nature* **429**, 771–776.
27 Okamura M, Inagaki T, Tanaka T & Sakai J (2010) Role of histone methylation and demethylation in adipogenesis and obesity. *Organogenesis* **6**, 24–32.
28 Pinnick KE & Karpe F (2011) DNA methylation of genes in adipose tissue. *Proc Nutr Soc* **70**, 57–63.
29 Isakson P, Hammarstedt A, Gustafson B & Smith U (2009) Impaired preadipocyte differentiation in human abdominal obesity: role of Wnt, tumor necrosis factor-alpha, and inflammation. *Diabetes* **58**, 1550–1557.
30 Gustafson B & Smith U (2012) The WNT inhibitor Dickkopf 1 and bone morphogenetic protein 4 rescue adipogenesis in hypertrophic obesity in humans. *Diabetes* **61**, 1217–1224.
31 Giovambattista A, Piermaría J, Suescun MO, Calandra RS, Gaillard RC & Spinedi E (2006) Direct effect of ghrelin on leptin production by cultured rat white adipocytes. *Obesity (Silver Spring)* **14**, 19–27.
32 Perello M, Castrogiovanni D, Giovambattista A, Gaillard RC & Spinedi E (2007) Impairment in insulin sensitivity after early androgenization in the post-pubertal female rat. *Life Sci* **80**, 1792–1798.
33 Giovambattista A, Chisari AN, Gaillard RC & Spinedi E (2000) Food intake-induced leptin secretion modulates hypothalamo-pituitary-adrenal axis response and hypothalamic Ob-Rb expression to insulin administration. *Neuroendocrinology* **72**, 341–349.
34 Giovambattista A, Gaillard RC & Spinedi E (2008) Ghrelin gene-related peptides modulate rat white adiposity. *Vitam Horm* **77**, 171–205.
35 Chen J, Dodson MV & Jiang Z (2010) Cellular and molecular comparison of redifferentiation of

intramuscular- and visceral-adipocyte derived progeny cells. *Int J Biol Sci* **6**, 80–88.
36 Chomczynski P & Sacchi N (2006) The single-step method of RNA isolation by acid guanidinium thiocyanate-phenol-chloroform extraction: twenty-something years on. *Nat Protoc* **1**, 581–585.
37 Grégoire F, Todoroff G, Hauser N & Remacle C (1990) The stroma-vascular fraction of rat inguinal and epididymal adipose tissue and the adipoconversion of fat cell precursors in primary culture. *Biol Cell* **69**, 215–222.
38 Maumus M, Sengene's C, Decaunes P, Zakaroff-Girard A, Bourlier V, Lafontan M, Galitzky J & Bouloumie A (2008) Evidence of in situ proliferation of adult adipose tissue-derived progenitor cells: influence of fat mass microenvironment and growth. *J Clin Endocrinol Metab* **93**, 4098–4106.
39 Moreno G, Perelló M, Camihort G, Luna G, Console G, Gaillard RC & Spinedi E (2006) Impact of transient correction of increased adrenocortical activity in hypothalamo-damaged, hyperadipose female rats. *Int J Obes (Lond)* **30**, 73–82.